Bonding and Structure of $TlGaSe_2$

Kyeong Ae Yee and Thomas A. Albright*

Contribution from the Department of Chemistry and Texas Center for Superconductivity at the University of Houston, University of Houston, Houston, Texas 77204-5641.
Received February 11, 1991

Abstract: The bonding and structure of $TlGaSe_2$ was investigated by tight-binding calculations with an extended Hückel Hamiltonian. The bonding between Tl and Se is found to be reasonably covalent, and the region around the Fermi level consists primarily of Tl 6s states antibonding to Se lone pairs. Two structural deformations have been proposed for the ferroelectricity associated with $TlGaSe_2$. One hypothesis involves a D_{2d} squashing motion of the Ga_4Se_4 adamantane unit. We find no evidence for a double-well potential, and the energy required for deformation is quite steep. On the other hand, a soft, double-well potential exists for the Tl atoms to slide away from a trigonal prismatic to a (3 + 3) environment. This in turn reinforces Tl-Tl bonding. The electronic factors that create this distortion are discussed and analyzed with the aid of a molecular and solid-state model.

Introduction

The ternary phases $TlBX_2$, where B = Ga and In and X = S, Se, and Te, have been known for sometime.[1] All are semiconductors and show good photoconductivity properties.[1h,2] At least four totally different structural types exist for these materials:[3] the TlSe (B37) type, the α-$NaFeO_2$ structure, a hexagonal modification, and $TlGaSe_2$[4] along with presumably $TlGaS_2$ and β-$TlInS_2$ form a unique structural type that will be the focus of this work. The latter three materials contain interesting structural elements that cause them to be ferroelectric. $TlGaSe_2$ was first discovered to undergo phase transitions in the region of 80-120 K.[5] Subsequent studies have shown that β-$TlInS_2$ underwent a phase transition at 196-215 K[6] and possibly $TlGaS_2$ at 115-118 K,[7] although some controversy concerning the latter exists.[5d,8] A large amount of data has been collected to investigate the phase transitions in especially $TlGaSe_2$ and β-$TlInS_2$. Heat capacity measurements,[5c,8,9] IR and Raman studies at low temperature,[4b,10] dielectric measurements,[10a,11] variable-temperature X-ray dif-

(1) (a) Hahn, H.; Wellmann, B. *Naturwissenschaften* **1967**, *54*, 42. (b) Müller, D.; Poltmann, F. E.; Hahn, H. *Z. Naturforsch.* **1974**, *29b*, 117. (c) Isaacs, T. J. *J. Appl. Crystallogr.* **1973**, *6*, 413. (d) Isaacs, T. J.; Hopkins, R. H. *J. Cryst. Growth* **1975**, *29*, 121. (e) Isaacs, T. J.; Feichtmer, J. D. *J. Solid State Chem.* **1975**, *14*, 260. (f) Gasanly, N. M.; Goncharov, A. F.; Melnik, N. N.; Ragimov, A. S.; Tagirov, V. I. *Phys. Status Solidi B* **1983**, *116*, 427. (g) Guseinov, G. D.; Ramazanzade, A. M.; Kerimova, E. M.; Ismailov, M. Z. *Ibid.* **1967**, *22*, K117. (h) Offergeld, G. R. U.S. Patent 3110685; *Chem. Abstr.* **1964**, *60*, 6325b.

(2) (a) Namedov, N. T.; Moroz, N. K. *Phys. Status Solidi B* **1990**, *159*, K83. (b) Nagat, A. T.; Gamal, G. A.; Hussein, S. A. *Phys. Status Solidi A* **1990**, *120*, K163. (c) Karpovich, I. A.; Chervova, A. A.; Leonov, E. I.; Orlov, V. M. *Ibid.* **1971**, *4*, K13. (d) Darvish, A. M.; Bakhyshov, A. E.; Tagirov, M. *Fiz. Tech. Poluprovodn.* **1977**, *11*, 780. Allakhverdiev, K. R.; Babaev, S. S.; Bakhyshov, N. A.; Mamedov, T. G. *Ibid.* **1984**, *18*, 1307. (e) Baltrameyunas, R.; Zhukaus, A.; Zeinalov, N.; Kuokshtis, E. *Ibid.* **1983**, *17*, 1898. (f) Guseinov, G. D.; Mustafayeva, S. N.; Bagirzade, E. F.; Abdullayev, E. G.; Guseinov, S. G. *Solid State Commun.* **1985**, *55*, 991. Guseinov, G. D.; Abdullaev, G. B.; Bidzinova, S. M.; Seidov, F. M.; Ismailov, M. Z.; Pashaev, A. M. *Phys. Lett. A* **1970**, *33*, 421. Guseinov, G. D.; Mustafaeva, S. N.; Guseinova, R. G. *Izv. Akad. Nauk SSR, Neorg. Mater.* **1989**, *25*, 150. (g) Karpovich, I. A.; Chervova, A. A.; Demidova, L. I.; Leonov, E. I.; Orlov, V. M. *Ibid.* **1972**, *8*, 70. (h) Samaras, I.; Kambas, K.; Julien, C. *Mater. Res. Bull.* **1990**, *25*, 1.

(3) (a) Range, K.-J.; Engert, G.; Müller, W.; Weiss, A. *Z. Naturforsch.* **1974**, *29b*, 181. (b) Range, K.-J.; Mahlberg, G.; Obenland, S. *Ibid.* **1977**, *32b*, 1374. (c) Müller, D.; Eulenberger, G.; Hahn, H. *Z. Anorg. Allg. Chem.* **1973**, *398*, 207. (d) Deiseroth, H.-J.; Müller, D.; Hahn, H. *Ibid.* **1985**, *525*, 163.

(4) (a) Müller, D.; Hahn, H. *Z. Anorg. Allg. Chem.* **1978**, *438*, 258. (b) Henkel, W.; Hochheimer, H. D.; Carlone, C.; Werner, A.; Ves, S.; von Schnering, H. G. *Phys. Rev. B* **1982**, *26*, 3211.

(5) (a) Allakhverdiev, K. R.; Nizametdinova, M. A.; Sardarly, R. M.; Vinogradov, E. A.; Zhinzhin, G. N. *Proceedings of the International Conference on Lattice Dynamics, Paris*; Flammarion: Paris, 1978; p 95. (b) Volkov, A. A.; Goncharov, Y. G.; Kozlov, G. V.; Lebedev, S. P.; Prokhorov, A. M.; Aliev, R. A.; Allakherdiev, K. R. *Sov. Phys. JETP Lett.* **1983**, *37*, 615. (c) Abdullaeva, S. G.; Abdullaev, A. M.; Mamedov, K. K.; Mamedov, N. T. *Sov. Phys. Solid State* **1984**, *26*, 375. (d) Aliev, R. A.; Allakhverdiev, K. R.; Baranov, A. I.; Ivanov, N. R.; Sardarly, R. M. *Ibid.* **1984**, *26*, 775. (e) Volkov, A. A.; Goncharov, Y. G.; Kozlov, G. V.; Allakhverdiev, K. R.; Sardarly, R. M. *Ibid.* **1983**, *25*, 2061.

(6) (a) Vakhrushev, S. B.; Zhdanova, V. V.; Kvyatkovskii, B. E.; Okuneve, N. M.; Allakhveriev, K. R.; Aliev, R. A.; Sardarly, R. M. *Sov. Phys. JETP Lett.* **1984**, *39*, 291. (b) Allakhverdiev, K. R.; Babaev, S. S.; Bakhyshov, N. A.; Mamedov, T. G. *Sov. Phys. Solid State* **1985**, *27*, 2230.

(7) Mal'sagov, A. U.; Kul'buzhev, B. S.; Khamkhoev, B. M. *Izv. Akad. Nauk SSSR. Neorg. Mater.* **1989**, *25*, 216.

(8) Mamedov, K. K.; Yangirov, A. Y.; Guseinov, A. G.; Abdullaev, A. M. *Phys. Status Solidi A* **1988**, *106*, 315.

(9) (a) Krupnikov, F. S.; Aliev, F. Y. *Sov. Phys. Solid State* **1988**, *30*, 1817. (b) Mamedov, K. K.; Abdullaev, A. M.; Kerimova, E. M. *Phys. Status Solidi A* **1986**, *94*, 115. (c) Allakhverdiev, K. R.; Mamedov, T. G.; Panfilov, V. V.; Skukyurov, M. M.; Subbotin, S. I. *Phys. Status Solidi B* **1985**, *131*, K23. Allakhverdiev, K. R.; Aldzanov, M. A.; Mamedov, T. G.; Salaev, E. Yu. *Solid State Commun.* **1986**, *58*, 295. (d) Aldzhanov, M. A.; Guseinov, N. G.; Mamedov, Z. N. *Phys. Status Solidi A* **1987**, *100*, K145. Viscakas, J. K.; Vaitkus, J. J.; Guseinov, G. D.; Abdullaeva, S. G.; Seidov, F. M.; Ismailov, M. Z.; Khalilov, Kh. J. *Mater. Res. Bull.* **1976**, *11*, 377. Aldzhanov, M. A.; Guseinov, N. G.; Mamedov, Z. N.; Abdurragimov, A. A. *Dokl. Akad. Nauk Az. SSR* **1987**, *43*, 23. (e) For a review see: Mamedov, K. K.; Yangirov, A. Yu.; Guseinov, A. G.; Abdullaev, A. M. *Phys. Status Solidi A* **1988**, *106*, 315.

(10) (a) Hochheimer, H. D.; Gmelin, E.; Bauhofer, W., von Schnering-Schwarz, C.; von Schnering, H. G.; Ihringer, J.; Appel, W. *Z. Phys. B: Condens. Mater.* **1988**, *73*, 257. (b) Allakhverdiev, K. R.; Babaev, S. S.; Tagiev, M. M.; Shirinov, M. M. *Phys. Status Solidi B* **1989**, *152*, 317. (c) Burlakov, V. M.; Ryabov, A. P.; Yakh'eev, M. P.; Vinogradov, E. A.; Melnik, N. N.; Gasanly, N. M. *Ibid.* **1989**, *153*, 727. Burlakov, V. M.; Vinogradov, E. A.; Gasanly, N. M.; Mel'nik, N. N.; Ryabov, A. P.; Yakh'eev, M. R. *Sov. Phys. Solid State* **1988**, *30*, 997; Burlakov, V. M.; Gasanly, N. M.; Yakh'eev, M. R. *Ibid.* **1990**, *32*, 29. Burlakov, V. M.; Nurov, Sh.; Ryabov, A. P. *Ibid.* **1989**, *30*, 2077. Burlakov, V. M.; Anikiev, A. A.; Yakh'eev, M. R. *Phys. Status Solidi B* **1990**, *161*, 883. Burlakov, V. M.; Yakh'eev, M. R. *Ibid.* **1989**, *151*, 337. Abdullaev, G. B.; Allakhverdiev, K. R.; Burakov, V. M.; Vinogradov, E. A.; Zhizhin, G. N.; Melnik, N. N.; Salaev, E. Yu.; Sardarly, R. M. *Dokl. Akad. Nauk Az. SSR* **1979**, *35*, 30. Burlakov, V. M.; Nurov, Sh.; Ryabov, A. P. *Fiz. Tverd. Tela (Leningrad)* **1988**, *30*, 3616. Agladze, N. I.; Antonyuk, B. P.; Burlakov, V. M.; Vinogradov, E. A.; Zhizhin, G. N. *Ibid.* **1981**, *23*, 3289. (d) Goncharov, Y. G.; Kozlov, G. V.; Kulbuzhev, B. S.; Shirokov, V. B.; Torgashev, V. I.; Volkov, A. A.; Yuzyk, Y. I. *Phys. Status Solidi B* **1989**, *153*, 529. Volkov, A. A. *Krystallografiya* **1985**, *30*, 1124; Volkov, A. A.; Goncharov, Yu. G.; Kozlov, G. V.; Sardarly, R. M. *Pis'ma Zh. Eksp. Teor. Fiz.* **1984**, *39*, 293. Volkov, A. A.; Goncharov, Yu. G.; Kozlov, G. V.; Torgashev, V. I.; Shirokov, V. B. *Fiz. Tverd. Tela (Leningrad)* **1988**, *30*, 3621. (e) Kul'buzhev, B. S.; Rabkin, L. M.; Torgashev, V. I.; Yuzyuk, Yu. I. *Ibid.* **1988**, *30*, 195. (f) Abdullaev, G. B.; Allakherverdiev, K. R.; Vinogradov, E. A.; Zhizhin, G. N.; Mel'nik, N. N.; Nani, R. Kh.; Salaev, E. Yu.; Sardarly, R. M. *Dokl. Akad. Nauk Az. SSR* **1977**, *33*, 26. (g) Abutalybov, G. I.; Salaev, E. Y. *Sov. Phys. Solid State* **1986**, *28*, 1231. (h) Gasanly, N. M.; Goncharov, A. F.; Melnik, N. N.; Ragimov, A. S.; Tagirov, V. I. *Phys. Status Solidi B* **1983**, *116*, 427. (i) Ibragimov, T. D.; Mamedov, N. T. *Phys. Status Solidi B* **1988**, *145*, K103.

(11) (a) Banis, Y.; Brilingas, A.; Grigas, I.; Guseinov, G. N. *Sov. Phys. Solid State* **1987**, *29*, 1906; Paprotnyi, V.; Grigas, I. *Ferroelectrics* **1985**, *65*, 201. Grigas, I.; Kalesinskas, V.; Paprotny, W.; Brilingus, A. *Jpn. J. Appl. Phys., Part 1* **1985**, *24*, 525. Brilingus, A.; Grigas, I.; Kalesinskas, V. *Izv. Akad. Nauk SSR, Ser.Fiz.* **1987**, *51*, 2196. (b) Volkov, A. A.; Goncharov, Y. G.; Kozlov, G. V.; Allakhverdiev, K. R.; Sardarly, R. M. *Sov. Phys. Solid State* **1984**, *26*, 1668, 2061. Allahverdiev, K. R.; Baranov, A. I.; Mamedov, T. G.; Sandler, V. A.; Sharifov, Y. N. *Ibid.* **1988**, *30*, 1007. Gashimzade, F. M.; Gadzhiev, B. R.; Allakhverdiev, K. R.; Sardarly, R. M.; Shteinshraiber, V. Ya. *Friz. Tverd. Tela (Leningrad)* **1985**, *27*, 2286. (c) Abiev, A. K.; Aliev, E. Z.; Natig, B. A.; Sardarly, R. M. *Phys. Status Solidi A* **1989**, *114*, K119.

0002-7863/91/1513-6474$02.50/0

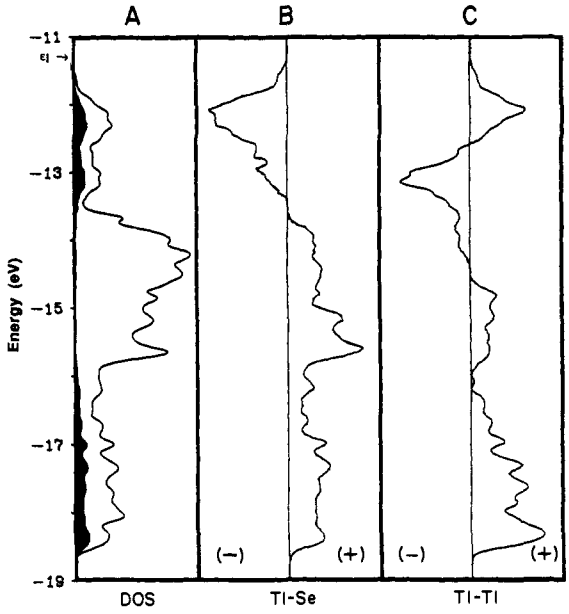

Figure 1. (A) Total density of states (DOS) in $TlGaSe_2$ (solid line). The blackened area corresponds to the projection of the Tl s orbitals. (B) Total projected Tl–Se COOP curve for $TlGaSe_2$. (C) Total projected Tl–Tl COOP curve for $TlGaSe_2$.

fraction,[10a,12] and NMR studies,[13] as well as other techniques,[14] have been thought to bear on this phenomena. Interestingly, there are oscillations of the heat capacity versus temperature around the phase-transition region,[9a] a devil's ladder, which has been interpreted[15] to arise from the intervention of incommensurate phases. No definitive evidence has been obtained about the nature of the displacive transition in $TlGaSe_2$ (and β-$TlInS_2$). Two proposals exist. Adopting a Zintl view of Se(2−) and Ga(3+), the oxidation state of Tl is formally 1+. Many years ago Orgel[16] predicted that distortions around a Tl(1+) environment would cause Tl 6p orbitals to mix into the filled Tl 6s level. The formation of directed lone pairs at Tl(1+) centers then creates a ferroelectric material. Drawing from this theory, von Schnering and co-workers[10a] have proposed a slippage of the Tl atoms in $TlGaSe_2$ to be at the heart of the displacive transition. On the other hand, Burlakov et al.[17] have concluded that the ferroelectric transition is created by angular deformations in the $GaSe_2$ tetrahedra.

In the present work we shall investigate the bonding in $TlGaSe_2$, particularly in the Tl–Se and Tl–Tl regions. Both structural models for the distortion will be examined and analyzed via discrete molecular and one-dimensional models. Our calculations are of the tight-binding type with an extended Hückel Hamiltonian.[18] Computational details are given in the Appendix. Previous band structure calculations[19] using a pseudopotential method have focused exclusively on the absorption spectra.

Prototype Structure

Before we begin our theoretical discussion, it is important to review the structural details. As mentioned previously, $TlGaSe_2$, $TlGaSe_2$, and β-$TlInS_2$ are isostructural although the atomic positional parameters of only $TlGaSe_2$ are known.[4] Crystals of $TlGaSe_2$ are monoclinic with C_2/c symmetry for the room-temperature, prototype structure. This can be regarded as a layered material. A view illustrating this feature in the *ac* plane is given in **1**. For visualization purposes, bonds between Tl and Se have

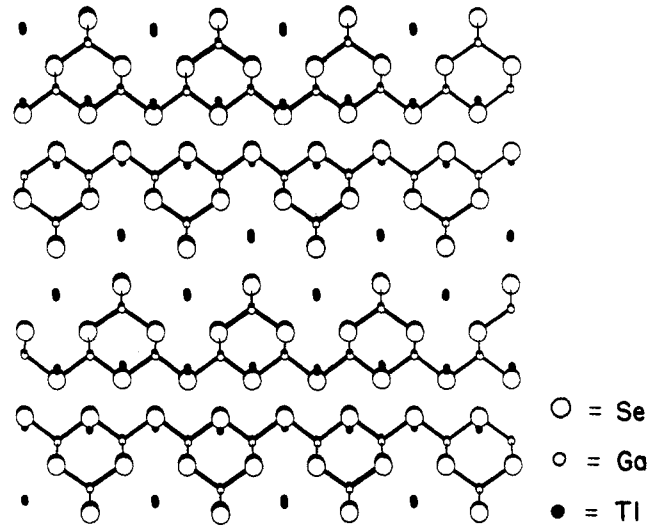

1

not been drawn. Each layer is stacked via a 4_2 screw mode. The $GaSe_2$ portion of the structure consists of Ga_4Se_6 adamantane-like units linked together in the *a* and *b* directions by bridging Se atoms. Each layer then has tetragonal symmetry, which is preserved upon cooling to low temperature.[10a] The Tl atoms are coordinated in a trigonal-prismatic manner; see **2**. The Tl–Se

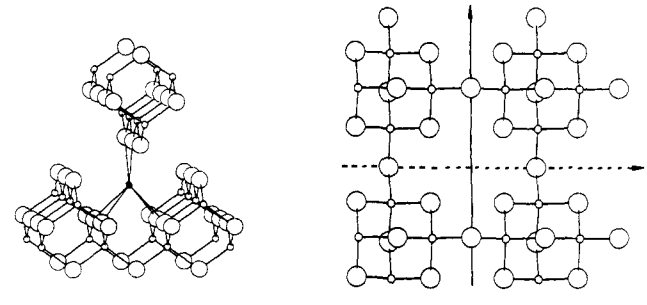

2 **3**

bond lengths[4] run from 3.23 to 3.50 Å with an average of 3.45 Å. The Tl atoms form nearly planar chains (Tl–Tl–Tl = 176.8–177.5°)[4] along the *a* and *b* directions. A representation of the structure in the *ab* plane is shown in **3**. The solid arrow represents the upper channel of Tl atoms while the broken one is for the lower channel in one layer. The Tl–Tl bond lengths are rather long, 3.79–3.83 Å, with an average of 3.81 Å. But this

(12) (a) Plyushch, O. B.; Sheleg, A. U.; Aliev, V. A.; Guseinov, G. D. *Sov. Phys. Solid State* **1989**, *31*, 1245. Aliev, V. A. *Kristallografiya* **1990**, *35*, 506. (b) Abdullaev, N. A.; Allakhverdiev, K. R. *Dokl. Akad. Nauk Az. SSR* **1985**, *41*, 21. (c) Mul'sagov, A. U.; Kul'buzhev, B. S.; Khamkhoev, B. M. *Izv. Akad. Nauk SSSR, Neorg. Mater.* **1989**, *25*, 216. Mul'sagov, A. U.; Berfirer, I. M.; Kul'buzhev, B. S. *Ibid.* **1989**, *25*, 375. (d) Barys, J.; Glazer, A. M.; Wondre, F. R. *Ferroelectrics* **1990**, *110*, 157.

(13) Panich, A. M. *Fiz. Tverd. Tela (Leningrad)* **1989**, *31*, 279. Mamedov, N. T.; Krupnikov, E. S.; Panich, A. M. *Ibid.* **1989**, *31*, 290. Panich, A. M.; Gabuda, S. P.; Mamedov, N. T.; Aliev, S. N. *Ibid.* **1987**, *29*, 3694.

(14) (a) Allakhverdiev, K. R.; Babirova, A. A.; Gadzhiev, B. R.; Mamedov, N. T. *Sov. Phys. Solid State* **1989**, *31*, 671. (b) Belyaev, A. D.; Galolobov, Yu. P.; Mamedov, T. G.; Sharifov, Ya. N. *Ukr. Fiz. Zh.* **1988**, *33*, 1705. (c) Laiho, R.; Sardarly, R. M. *Ferroelectrics* **1987**, *80*, 185. (d) Abdullaeva, S. G.; Mamedov, N. T. *Fiz. Tverd. Tela (Leningrad)* **1986**, *28*, 894. Abdullaeva, S. G.; Mamedov, N. T.; Mamedov, Sh. S.; Mustafaev, F. A. *Ibid.* **1987**, *29*, 3147.

(15) Volkov, A. A.; Goncharov, Yu. G.; Lebedev, S. P.; Prokhorov, A. M.; Aliev, R. A.; Allakhverdiev, K. R. *Zh. Eksper. Teor. Fiz. Pisma* **1983**, *37*, 517. Vakhrushev, S. B.; Zhdanova, V. V.; Kvyatkovski, B. E.; Okuneva, M. M.; Allakhverdiev, K. R.; Aliev, R. A.; Sardarly, R. M. *Ibid.* **1984**, *39*, 245. Aliev, R. A.; Allakhverdiev, K. R.; Baranov, A. I.; Ivanov, A. I.; Sardarly, R. M. *Fiz. Tverd. Tela (Leningrad)* **1984**, *26*, 1271.

(16) Orgel, L. E. *J. Chem. Soc.* **1959**, *4*, 3815.

(17) Burlakov, V. M.; Nurov, S.; Ryabov, A. P. *Sov. Phys. Solid State* **1988**, *30*, 2077.

(18) (a) Hoffmann, R. *J. Chem. Phys.* **1963**, *39*, 1397. (b) Hoffmann, R.; Lipscomb, W. N. *Ibid.* **1962**, *36*, 2179. (c) Whangbo, M.-H.; Hoffmann, R.; Woodward, R. B. *Proc. R. Soc. London, Ser. A* **1979**, *366*, 23.

(19) (a) Abdullaeva, S. G.; Mamedov, N. T. *Phys. Status Solidi B* **1986**, *133*, 171. (b) Abdullaeva, S. G.; Mamedov, N. T.; Orudzhev, G. S. *Ibid.* **1983**, *119*, 41.

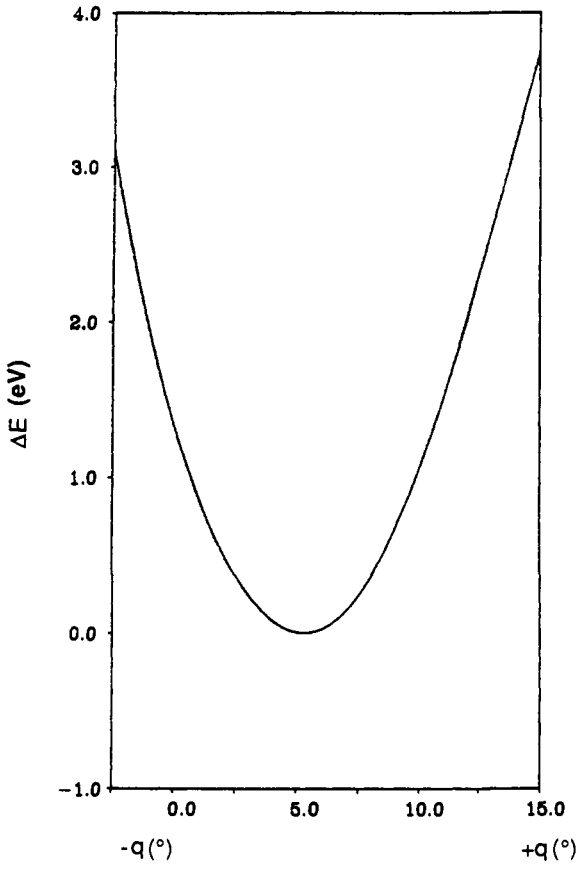

Figure 2. Computed total energy difference per unit cell for the distortion coordinate (q) defined in **4**.

is still in the range of many other Tl-based solid-state structures where it has been argued[20] that some reminants of Tl–Tl bonding exists.

Bonding in $TlGaSe_2$

A single layer of the $GaSe_2^-$ adamantane units is considered. In a localized sense two s and p hybrids on Se are utilized to form σ bonds to four Ga s and p hybrids. Thus, at low energy the filled orbitals are Ga–Se bonding and centered on the more electronegative Se atoms. At high energy the empty orbitals are Ga–Se antibonding and more localized on Ga. There is a very large energy gap between these two regions indicative of strong covalent bonding. Below the Fermi level, from −13.2 to −16.3 eV, are the lone pairs on the Se atoms. One lone pair is an s and p hybrid that lies in the Ga–Se–Ga plane and the other is in a p orbital orthogonal to this plane. When one does a calculation on the Tl^+ atoms by themselves, where the positions are taken from the structure of $TlGaSe_2$, the filled Tl s states lie in a region from −14.5 to −18.2 eV. The empty Tl p orbitals span a very large range from −1.2 to −11.5 eV. The large dispersion of the atomic orbitals signals some Tl–Tl communication in our calculations.

Figure 1A shows the resultant density of states (DOS) for $TlGaSe_2$. The projection of Tl s states is shown by the darkened area under the total DOS (solid line). The Tl s region is split into two portions, one from ~−15.5 to −18.7 eV and the other from −11.3 to ~−13.5 eV. The projection of the Tl–Se crystal orbital overlap population[21] (COOP) is given in Figure 1B. The lower energy Tl s region is Tl–Se bonding while the higher energy portion is Tl–Se antibonding. Notice from the position of the Fermi level, ϵ_F, in Figure 1A, that all of these orbitals are filled. Then is the Tl–Se interaction repulsive? The empty Tl p orbitals are greatly destabilized after interaction. These orbitals also mix with the Se lone pairs and create a net bonding situation especially in the region from ~−13.6 to −16.0 eV. Numerically, Tl–Se interaction is, in fact, antibonding with a net overlap population of −0.026 when Tl p orbitals are deleted from the calculation. However, the overlap population becomes positive (0.068) when they are included. The Tl p orbitals also play a decisive role in the Tl–Tl interaction. Without p orbitals the Tl–Tl overlap population is −0.006. However, when they are added, the overlap population rises to 0.065. The Tl–Tl COOP curve is presented in Figure 1C. Notice that in the lower energy region there is predominantly Tl–Tl bonding while in the upper portion the bonding and antibonding components approximately cancel. We will have much more to say about this situation in the next section.

The global pattern that then emerges is very strong, covalent bonding between Ga and Se. Tl–Se and Tl–Tl interactions exist and are rendered to be net bonding via the intervention of Tl p orbitals. The Fermi level is dominated by Tl s and Se lone pair combinations, which are antibonding. Our indirect band gap of 3.2 eV is larger than that from pseudopotential calculations reported by Abdullaeva and co-workers[19] (2.1 eV). Experimentally, it has been measured to be about 2.25 eV.[22,23]

Nature of the Ferroelectric Distortion

As mentioned in the Introduction, two proposals have been made for the atomic deformations at the ferroelectric transition point. The $GaSe_2$ adamantane-like portion of the structure possesses local D_{2d} symmetry. Burlakov, Nurov, and Ryabov have suggested[17] a breathing mode in the Ga_4Se_6 unit, shown in **4**. This reduces

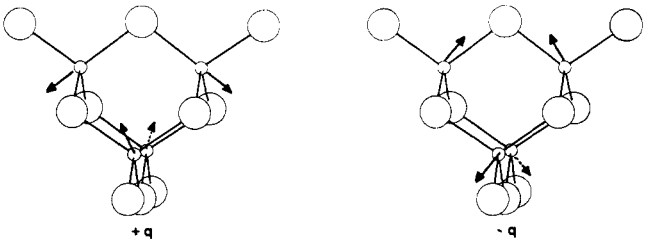

4

the local symmetry to C_2; hence, an inversion center is lost. The distortion coordinate (q) involves changing the Se–Ga–Se (and Ga–Se–Ga) angles so that when $q = 0$ all Se–Ga–Se angles are tetrahedral. This deformation mode was investigated, keeping the Ga–Se and Tl–Se distances constant. The results are presented in Figure 2. A minimum was found for $q = +5°$, which is, in fact, close to the experimental structure.[4] The curvature in either direction is quite steep in keeping with strongly covalent Ga–Se bonding. For this reason, slippage of the Ga or Se from their positions is not expected to yield a soft vibrational mode. A ferroelectric material must have two or more orientational (conformational) states in the absence of an electric field, which can be shifted from one to another by an electric field. There is no evidence for the existence of a double-well potential. Therefore, our calculations do not agree with the proposal that this is the source of the displacive mode in $TlGaSe_2$. On the other hand, von Schnering and co-workers suggested[10a] that the Tl atoms along the channels in the a and b directions (see **3**) slip from their trigonal-prismatic environments to a (3 + 3) coordination mode as shown in **5**. An inversion center is then lost, and the space

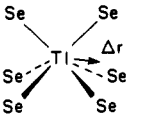

5

group changes from $C2/c$ to Cc. Starting from a structure where

(20) Janiak, C.; Hoffmann, R. *J. Am. Chem. Soc.* **1990**, *112*, 5924.
(21) Hoffmann, R. *Solid and Surfaces: A Chemist's View on Bonding in Extended Structures*; VCH: New York, 1988.
(22) Aliev, V. A.; Nadzhafov, A. I. *Dokl. Akad. Nauk Az. SSSR* **1981**, *37*, 33.
(23) A smaller band gap is found in: Abdullaeva, S. G.; Belenskii, G. L.; Godzhaev, M. O.; Mamedov, N. T. *Phys. Status Solidi B* **1983**, *103*, K61.

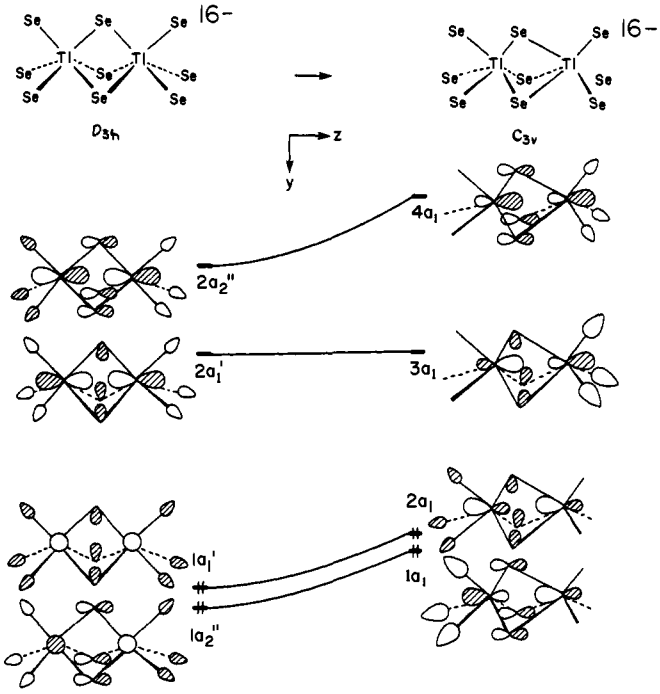

Figure 3. Walsh diagram for Tl slippage in $Tl_2Se_9^{16-}$.

the Tl–Se distances are at their averaged experimental values,[4] slippage of the Tl atoms, measured by Δr, lowers the computed total energy. Since slippage is equivalent in either direction, this creates a double-well potential. Our optimized value of $\Delta r = 0.80$ Å with an energy lowering of 2.5 kcal/mol per formula unit is probably an overestimate.[24] A value of $\Delta r = 0.30$ Å has been proposed in the literature,[10a] which amounts in our calculations to a 1.8 kcal/mol stabilization per formula unit. Before we examine the electronic sources of this distortion, we will first treat two prototypical situations.

The hypothetical $Tl_2Se_9^{16-}$ molecule, **6**, represents the most simple example that preserves the Tl–Se and Tl–Tl environments. Figure 3 presents a Walsh diagram for Tl slippage in this molecule.

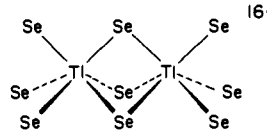

6

On the left side are the two highest occupied and lowest unoccupied molecular orbitals at the undistorted, D_{3h}, geometry (Tl–Se = 3.45 Å; Tl–Tl = 3.90 Å). The $1a_2''$ and $1a_1'$ molecular orbitals are primarily Tl s in character antibonding to the surrounding Se atoms. Notice that the Tl–Tl in-phase combination ($1a_1'$) is at a higher energy than the Tl–Tl out-of-phase member ($1a_2''$). This is due to greater Tl–Se antibonding from the bridging Se atoms in the former molecular orbital. There are, of course, Tl–Se bonding counterparts to $1a_1'$ and $1a_2''$ that are occupied and lie at lower energies. The two lowest unoccupied molecular orbitals, $2a_1'$ and $2a_2''$, are Tl p-based combinations. When the Tl atoms move to the right, along the z direction in this figure, two important perturbations[25] occur. The energy rises in first order since the antibonding increases more to the Se atoms with shorter Tl–Se distances than it decreases to those with longer Tl–Se bond lengths.[26] What is equally important is that the Tl–Se bonding counterparts to $1a_2''$ and $1a_1'$ are stabilized for the same reason. But there is also a second-order perturbation at work here. Empty $2a_2''$ and $2a_1'$ mix into $1a_1'$ and $1a_2''$, respectively, with the relative phases shown on the left side of Figure 2. This intermixing is stabilizing; i.e., it keeps $1a_1'$ and $1a_2''$ (now $1a_1'$ and $2a_1'$ in the reduced, C_{3v}, symmetry of the distorted structure) from rising too high in energy. Hybridized lone pairs are formed pointing in the direction opposite to the Tl atom slippage. In our calculations, the optimized structure is one with the Tl atoms slipped 0.57 Å and the total energy is lowered by 4.1 kcal/mol. At the D_{3h} geometry, the percent Tl p character in $1a_1'$ and $1a_2''$ is 2.5% and 1.4%, respectively, whereas, at the optimized structure, the $2a_1$ and $1a_1$ molecular orbitals have 26.6% and 29.4% Tl p character.

There are two further ramifications for the increased Tl p mixing into the occupied molecular orbitals. First, Tl p mixes into $1a_1'$ and $1a_2''$ in a bonding way to the facial Se_3 ligand sets, which have a shorter Tl–Se distance. Consequently, the net Tl–Se bonding to these atoms is increased when the Tl atoms slip. Second, Janiak and Hoffmann[20] have shown in detail that Tl(1+)–Tl(1+) interactions in molecular and solid-state systems can be turned into a net bonding situation by Tl p mixing into filled Tl s orbitals. The same situation applies here for identical reasons; the Tl–Tl overlap population increases from 0.058 at D_{3h} to 0.095 at the optimized structure. Notice that the Tl–Tl distance is not changed along the distortion coordinate. This is exclusively an effect due to increased Tl p mixing.

An alternative approach to this problem is to consider a $TlSe_3^{5-}$ one-dimensional chain **7**. Figure 4 shows the band structures for an undistorted (dotted line) and the optimized, $\Delta r = 0.73$ Å, structure (solid line). The highest occupied band in the figure

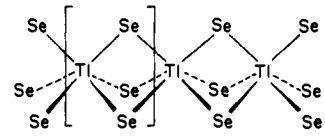

7

is labeled $2a_1$. Its functional form at the zone center (Γ) is identical with $1a_1'$ and $1a_1$ for the undistorted and distorted structures, respectively, in Figure 3. Likewise, at the zone edge (Z) the $2a_1$ band strongly resembles $1a_2''$ and $2a_1$. Notice that the band runs down in energy going from Γ to Z for precisely the same reasons that molecular $1a_1'$ is higher in energy than $1a_2''$. The band labeled $3a_1$ in Figure 4 is primarily Tl p along the chain direction. It should come as no surprise that Tl slippage along the channel destabilizes the $2a_1$ band while several lower bands are stabilized. What stops the $2a_1$ band from being pushed up too high in energy and renders net stabilization for this distortion is the $3a_1$ band. It mixes into $2a_1$ to create lone pair hybrids at Tl. An increase in Tl–Se and Tl–Tl bonding is also evident; for example, the Tl–Tl overlap population increases from 0.056 to 0.137 going from the undistorted to the $\Delta r = 0.73$ Å structure.

We are now at a position to return to $TlGaSe_2$. The region near the Fermi level, from −11.3 to ~−13.5 eV (see Figure 1A) is dominated by pseudo-one-dimensional Tl s bands topologically analogous to the $2a_1$ band in Figure 4.[27] The lower portion of this region is Tl s–Tl s antibonding. States analogous to $1a_2''$ in Figure 3 are present. The higher energy portion is Tl s–Tl s bonding where states of the form of $1a_1'$ (in Figure 3) are found. This precisely matches the behavior of Tl–Tl (COOP) curve in Figure 1C from −11.3 to −13.5 eV.

As mentioned previously, we find an optimized value of 0.80 Å for Tl atom slippage along the channels in $TlGaSe_2$. Just as in the previous examples, the mixing of virtual Tl p states into orbitals around the Fermi level is absolutely critical for this process.

(24) The extended Hückel method frequently predicts bond lengths that are too short. See: Calzaferri, G.; Forss, L.; Kamber, I. *J. Phys. Chem.* **1989**, *93*, 5366.

(25) For a description of perturbation theory, see: Albright, T. A.; Burdett, J. K.; Whangbo, M.-H. *Orbital Interactions in Chemistry*; Wiley: New York, 1985.

(26) The overlap of Tl s to the Se combinations varies in an exponential fashion with respect to the Tl–Se distance. A dramatic example of this effect is given in the bands labeled 5e in Figure 4. They are destabilized by ~1.5 eV upon Tl slippage.

(27) Full details of the band structure calculations for $TlGaSe_2$ may be found in: Yee, K. A. Ph.D. Dissertation, University of Houston, 1990.

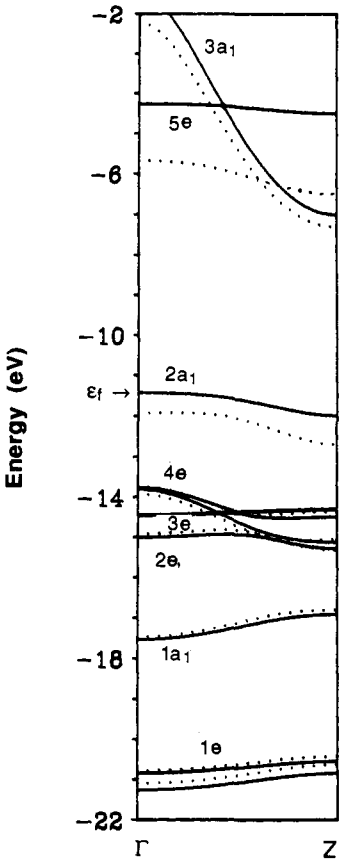

Figure 4. Band structure for the $TlSe_3^{5-}$ chain at the prototype (dotted lines) and the optimized (solid lines) geometry for Tl slippage. At Γ $k = 0$, and at Z $k = \pi/a$.

The intermixing provides the driving force to create the double-well potential. Hybridized lone pairs are created that point in the opposite direction to Tl slippage. A unique consequence is that Tl–Tl bonding (communication) is increased although the Tl–Tl distance remains constant. The total Tl–Tl overlap population increases from 0.065 to 0.105 upon going from the prototype to the optimized structure.[28] There are three, albeit indirect, pieces of information in accord with our hypothesis. First, we mentioned previously that Tl slippage reinforces Tl–Se bonding to the facial Se_3 set with shorter Tl–Se distances. In our calculations, the Tl–Se overlap population increases from 0.068 at the prototype to 0.237 at the optimized geometry.[29] The interlayer distance, $c \sin \beta$, should and does[10a,30] markedly decrease at the transition temperature. On the other hand, the a (and b) parameter shows a minor increase at T_c. Second, referring back to **3**, it was of interest to explore whether or not slippage of Tl atoms in the a direction is connected with (induces or retards) Tl atom slippage in the b direction. There is certainly no direct communication. The shortest Tl–Tl contact between the two channels is 4.38 Å;[4] however, this might occur through bond coupling in the Ga–Se framework. In our calculations, slippage of Tl atoms in the channels parallel to the a direction while the Tl atoms remained fixed in the channels parallel to the b direction, and vice versa, resulted in an energy lowering of half (within 0.04 kcal/mol per formula unit) of the total energy. Thus, slippage in either direction is predicted to be not strongly correlated. This may explain the existence of a devil's ladder in the heat capacity versus temperature measurements;[9a] incommesure phases may be formed via noncorrelated Tl slippages. Third, we have shown that the Tl lone pairs move to higher energy upon slippage for both the molecular (Figure 3) and one-dimensional (Figure 4) models. In $TlGaSe_2$ the Fermi level rises from −11.5 to −11.2 eV on going from the prototype to optimized structure. The indirect band gap is then computed to decrease from 3.2 to 2.7 eV. As mentioned previously, the band gap at 300 K has been measured at 2.25 eV.[22] The indirect band gap at 1.8 K was reported to be 2.17 eV.[31] This trend is in agreement with our calculations although more work is clearly needed. Likewise, we encourage a determination of the crystal structure at a temperature below the ferroelectric distortion to check on the central premise that Tl slippage to a (3 + 3) coordination mode is at the heart of the ferroelectric displacement.

Table I. Parameters Used for the Calculations

atom	orbital	H_{ii} (eV)	ζ
Tl	6s	−16.20	2.37
	6p	−9.00	1.97
Ga	4s	−14.58	1.77
	4p	−6.75	1.55
Se	4s	−20.50	2.44
	4p	−14.40	2.07

Appendix

Tight-binding calculations with an extended Hückel Hamiltonian[18] were used for all calculations. The atomic parameters[32] are listed in Table I. The geometry for $TlGaSe_2$ (as well as for the $Tl_2Se_9^{16-}$ molecule and $TlSe_3^{5-}$ chain) were averaged values from the X-ray structure.[4a] For the $TlSe_3^{5-}$ chain a 50 K point set was used along with a 96 K point set for $TlGaSe_2$ with the values chosen according to a literature method.[33]

Acknowledgment. We thank the Robert A. Welch Foundation, Petroleum Research Fund, administered by the American Chemical Society, and Texas Center for Superconductivity at the University of Houston (Prime Grant MDA 972-88-G-0002 from the Defense Advanced Research Projects Agency and the State of Texas) for support of this work. We also thank the NSF for a generous allocation of computer time at the Pittsburgh Supercomputer Center.

Registry No. $TlGaSe_2$, 12160-62-2.

(28) It has been convincingly argued (see ref 13) that the ^{203}Tl and ^{205}Tl NMR lines widths increase greatly upon lowering the temperature and that this is due to increased overlap between the Tl orbitals in the chains rather than environmental changes in the incommesurate phase(s).

(29) The three Tl–Se distances that become longer are rendered nonbonding. The overlap population decreases from 0.068 to −0.013.

(30) Aliev, V. A. *Sov. Phys. Crystallogr.* **1990**, *35*, 293.

(31) (a) Abutalybov, G. I.; Neimanzade, I. K.; Razbirin, B. S.; Salaev, E. Y.; Starukhin, A. N. *Fiz. Tekh. Poluprovodn.* **1986**, *20*, 1699. (b) Abutalybov, G. I.; Akopyan, I. Kh.; Neimanzade, I. K.; Novikov, B.; Salaev, E. Y. *Sov. Phys. Solid State* **1985**, *27*, 2836.

(32) (a) Kang, D. B.; Jung, D.; Whangbo, M.-H. *Inorg. Chem.* **1990**, *29*, 257. (b) Canadell, E.; Eisenstein, O.; Rubio, J. *Organometallics* **1984**, *3*, 759. (c) Hoffmann, R.; Shaik, S.; Scott, J. C.; Whangbo, M.-H.; Foshee, M. J. *J. Solid State Chem.* **1980**, *34*, 263.

(33) Ramirez, R.; Böhm, M. C. *Int. J. Quantum Chem.* **1986**, *30*, 391; *Ibid.* **1988**, *34*, 571.